Effect of epidemic spreading on species coexistence in spatial rock-paper-scissors games

Wen-Xu Wang,[1] Ying-Cheng Lai,[1,2,3] and Celso Grebogi[3]
[1]*School of Electrical, Computer, and Energy Engineering, Arizona State University, Tempe, Arizona 85287, USA*
[2]*Department of Physics, Arizona State University, Tempe, Arizona 85287, USA*
[3]*Institute for Complex Systems and Mathematical Biology, King's College, University of Aberdeen, Aberdeen AB24 3UE, United Kingdom*
(Received 5 January 2010; revised manuscript received 2 April 2010; published 23 April 2010)

A fundamental question in nonlinear science and evolutionary biology is how epidemic spreading may affect coexistence. We address this question in the framework of mobile species under cyclic competitions by investigating the roles of both intra- and interspecies spreading. A surprising finding is that intraspecies infection can strongly promote coexistence while interspecies spreading cannot. These results are quantified and a theoretical paradigm based on nonlinear partial differential equations is derived to explain the numerical results.

DOI: 10.1103/PhysRevE.81.046113 PACS number(s): 89.65.−s, 87.23.Cc, 02.50.Ey, 05.45.−a

Understanding the dynamical and physical mechanisms that facilitate or hamper biodiversity is a fundamental issue in interdisciplinary science. Species coexistence is key to maintaining biodiversity. Recently, a powerful theoretical and computational paradigm in nonlinear science has emerged, namely, evolutionary games, allowing for the first time the species-coexistence problem on spatially extended scales to be addressed quantitatively [1–6]. The development of the evolutionary-game approach was largely motivated by experiments on the role of nonhierarchical, cyclic competitions in coexistence. Exemplary biophysical systems where such competitions have been observed in several ecosystems [1,7–9]. For such systems, the coevolutionary dynamics can be well captured by the *rock-paper-scissor* game [5].

Quite recently, a basic feature of ecosystems, namely, population mobility, has been incorporated into spatial cyclic-competition games [10,11]. In the work of Reichenbach *et al.* [11], a critical mobility was identified, below which species can coexist, as manifested by patterns of entangled traveling spiral waves. Subsequently, issues such as noise and correlation [12,13], instability of spatial patterns [14], conservation law [15], and basin of biodiversity [16] were studied. In all these works, a main result is that, when the mobility exceeds a critical value, extinction arises in general, leading to the loss of coexistence. An intriguing implication of this result is that, about the critical value, the species differing slightly in mobility can have drastically different outcomes, leading to either existence or extinction. An important fact is, however, that species coexistence is such a ubiquitous phenomenon in nature. It is not unreasonable to conceive that species of relatively large mobility can coexist in certain environments. There must then be additional mechanisms that promote coexistence even when the species are highly mobile. The purpose of this paper is to establish that epidemic spreading can greatly enhance coexistence.

Epidemic spreading and outbreak are common in nature and society. The dynamics of spreading has been studied extensively on various networks [17]. However, the effects of virus spreading have not been addressed in the framework of evolutionary games. There are two spreading types: intra- and interspecies. Intraspecies virus spreading is extremely common, while the occurrence of interspecies spreading has become increasingly frequent, such as SARS, bird flu, and swine flu. Here we incorporate epidemic spreading into spatial game of mobile populations under cyclic competitions. Our main finding is that intraspecies spreading can strongly promote coexistence even when the species have high mobility. In particular, depending on parameters characterizing spreading, in a proper state space intraspecies spreading can generate a significant basin of coexistence. We will show that this striking finding can be explained by the underlying theory of nonlinear dynamics. We will derive a theoretical framework to treat both types of spreading based on a set of nonlinear partial differential equations (PDEs). Our findings elucidate the fundamental role played by virus spreading in species coexistence, which may have significant implications in ecosystems.

Cyclic-competitions. Cyclic-competitions of three mobile species, as proposed in Ref. [11], are modeled as follows:

$$ab \xrightarrow{u} a\varnothing, \quad bc \xrightarrow{u} b\varnothing, \quad ca \xrightarrow{u} c\varnothing, \tag{1}$$

$$a\varnothing \xrightarrow{\sigma} aa, \quad b\varnothing \xrightarrow{\sigma} bb, \quad c\varnothing \xrightarrow{\sigma} cc, \tag{2}$$

$$a\odot \xrightarrow{\varepsilon} \odot a, \quad b\odot \xrightarrow{\varepsilon} \odot b, \quad c\odot \xrightarrow{\varepsilon} \odot c, \tag{3}$$

where a, b, and c denote individuals from three species, respectively, $\varnothing$ represents empty sites and $\odot$ represents any species or empty sites. Relations (1)–(3) define prey, reproduction, and migration that occur at the rates u, σ, and ε, respectively. According to Ref. [11], the occurring probabilities of the three relations are normalized by the sum of the probabilities. Without loss of generality, we assume $u=\sigma=1$ [11]. Individual mobility M is defined [18] as $M=\varepsilon(2N)^{-1}$, which is proportional to the number of sites explored by one mobile individual per time step. Initially, three species populate a square lattice of N sites with periodic boundary conditions. At each time step, a random pair of neighboring sites is chosen for possible interaction, and one interaction from prey, reproduction and migration will occur, depending on their probabilities. Whether the interaction can successfully occur is determined by the states of both sites. An actual time step is defined when each indi-

vidual has experienced interaction once on average, i.e., in one time step N pairwise interactions will have occurred.

Epidemic spreading. This process is independent of cyclic competitions. We use the standard susceptible-infected-dead model to describe the process, where each individual can be in one of the three states: susceptible ($S_{a,b,c}$), infected ($I_{a,b,c}$), or dead. Virus is transmitted and spread in space through contact among neighboring individuals. Intra- and interspecies infections are described, as follows:

$$I_a S_a \xrightarrow{\lambda} I_a I_a, \quad I_b S_b \xrightarrow{\lambda} I_b I_b, \quad I_c S_c \xrightarrow{\lambda} I_c I_c, \tag{4}$$

$$\text{Ⓘ}\,\text{Ⓢ} \xrightarrow{\lambda} \text{Ⓘ}\,\text{Ⓘ}, \tag{5}$$

where Ⓘ and Ⓢ represent infected and susceptible individuals in any of the three species. Relation (4) stands for intraspecies infection with probability λ and relation (5) for interspecies infection by which virus can spread both within and across species with probability λ. A direct consequence of infection is death with probability δ: $\text{Ⓘ} \xrightarrow{\delta} \varnothing$, which occurs to any infected individuals for both intra- and interspecies infections. The infection process is updated synchronously at each actual time step t. At an arbitrary time t after the infection, individuals infected at or early than $t-1$ can die with probability δ. Either intra- or interspecies infections can occurs in population and the situation that both arise is not considered.

To guide our computations, we use one result in Ref. [11], where a critical mobility $M_c=(4.5\pm0.5)\times10^{-4}$ was identified. In the absence of virus spreading, for $M>M_c$, only one species can survive, so coexistence is ruled out. To effectively reveal the role of spreading in coexistence, it is then useful to distinguish two regimes: $M>M_c$ and $M<M_c$. Figures 1(a)–1(d) show typical snapshots of spatial pattern for different values of λ and δ, where Figs. 1(a)–1(c) are for intraspecies and Fig. 1(d) is for interspecies spreading. In particular, Fig. 1(a) demonstrates entangled moving spiral waves for $M<M_c$ for relatively small values of λ and δ, similar to what happens in the absence of infection spreading [11]. For relatively larger values of λ and δ, spiral-wave patterns become less pronounced, as shown in Fig. 1(b). Figure 1(c) exemplifies the spatial pattern for $M>M_c$, where color dots spread out uniformly, indicating stable coexistence, in sharp contrast to the case of no virus spreading, where coexistence cannot occur. However, for interspecies spreading, extinctions still occur for $M>M_c$, while for $M<M_c$, spiral waves are preserved but there are a large number of empty sites caused by interspecies infection for small values of λ and δ, as shown in Fig. 1(d). For large values of λ and δ, spiral-wave patterns are blurred, similar to the case of intraspecies spreading. All these patterns can be obtained theoretically by deriving and solving a set of PDEs [Eq. (7)], as shown in Figs. 1(e)–1(h).

The numerically obtained spiral-wave patterns can in fact be predicted theoretically by using nonlinear PDEs [11,13]. Let $I_{a,b,c}(\mathbf{r},t)$ and $S_{a,b,c}(\mathbf{r},t)$ be the infection and susceptible densities of populations a, b, and c at time t and spatial site $\mathbf{r}=(r_1,r_2)$. Neighbors are located at $\mathbf{r}\pm\delta r\cdot\mathbf{e}_i$, where $\{\mathbf{e}_i\}$ is

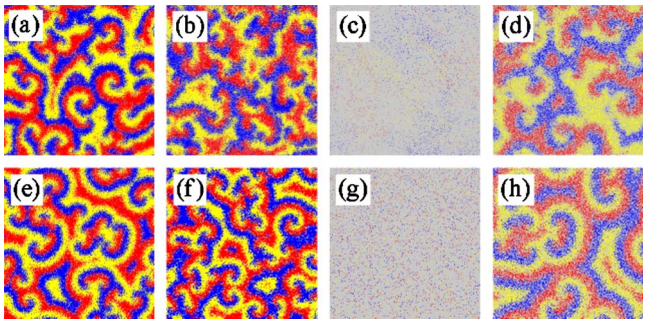

FIG. 1. (Color online) (a–c) Examples of spatial patterns under intraspecies spreading. Parameters are: (a) $M=2\times10^{-5}<M_c$, λ=0.02, and δ=0.01, (b) $M=2\times10^{-5}$, λ=0.1, and δ=0.05, and (c) $M=1\times10^{-3}>M_c$, λ=0.8, and δ=0.05. (d) Pattern in the presence of interspecies spreading for $M=2\times10^{-5}<M_c$, λ=0.2, and δ=0.05. (e–f) Corresponding theoretical patterns predicted by Eq. (7). The lattice size is 400×400. In the simulation patterns, three colors represent three species and gray is for empty site. The color of each site is the species of the individual who occupies the site. In the theoretical patterns, the color of a site is determined by the densities of three species probabilistically, that is the probability of showing a color at a site is proportional to the density of the species represented by the color. The densities of three species at a site in theoretical model is obtained by numerically solving Eq. (7). The time series of densities in (c) and (g) are quite stable with small fluctuations about their respective mean values, signifying coexistence induced by intraspecies virus spreading.

the basis of two-dimensional lattice. The quantities $\rho_{a,b,c}(\mathbf{r},t)=I_{a,b,c}(\mathbf{r},t)+S_{a,b,c}(\mathbf{r},t)$ represent the densities of the three species at position $\mathbf{r}$ and time t, and $\rho(\mathbf{r},t)=\rho_a(\mathbf{r},t)+\rho_b(\mathbf{r},t)+\rho_c(\mathbf{r},t)$ is the total density at $(\mathbf{r},t)$. The parameters $\alpha=\lambda/(\varepsilon+u+\sigma)$ and $\beta=\delta/(\varepsilon+u+\sigma)$ are the rescaled probabilities of infection and death. We then obtain the following evolutionary equations for any one of populations, say:

$$\begin{aligned}\partial_t I_a(\mathbf{r},t) = \frac{1}{4}\sum_{i\in 2D}\{2\epsilon[I_a(\mathbf{r}\pm\delta r\cdot\mathbf{e}_i,t)-I_a(\mathbf{r},t)]+\alpha\psi_a S_a(\mathbf{r},t)\\ -\beta I_a(\mathbf{r},t)-uI_a(\mathbf{r},t)\rho_c(\mathbf{r}\pm\delta r\cdot\mathbf{e}_i,t)\},\end{aligned}$$

$$\begin{aligned}\partial_t S_a(\mathbf{r},t) = \frac{1}{4}\sum_{i\in 2D}\{2\epsilon[S_a(\mathbf{r}\pm\delta r\cdot\mathbf{e}_i,t)-S_a(\mathbf{r},t)]-\alpha\psi_a S_a(\mathbf{r},t)\\ -uS_a(\mathbf{r},t)\rho_c(\mathbf{r}\pm\delta r\cdot\mathbf{e}_i,t)\\ +\sigma\rho_a(\mathbf{r}\pm\delta r\cdot\mathbf{e}_i,t)[1-\rho(\mathbf{r},t)]\},\end{aligned} \tag{6}$$

where for intra- and interspecies transmissions, $\psi_{a,b,c}=I_{a,b,c}(\mathbf{r}\pm\delta r\cdot\mathbf{e}_i,t)$ and $\psi_{a,b,c}=I_a(\mathbf{r}\pm\delta r\cdot\mathbf{e}_i,t)+I_b(\mathbf{r}\pm\delta r\cdot\mathbf{e}_i,t)+I_c(\mathbf{r}\pm\delta r\cdot\mathbf{e}_i,t)$, respectively. For $N\to\infty$ and lattice size fixed at one, $\delta r\to0$. Thus, $\mathbf{r}$ can be treated as a continuous variable. Using the expansion for $I_a(\mathbf{r}\pm\delta r\cdot\mathbf{e}_i,t)$ [similar for $S_a(\mathbf{r}\pm\delta r\cdot\mathbf{e}_i,t)$]: $I_a(\mathbf{r}\pm\delta r\cdot\mathbf{e}_i,t)=I_a(\mathbf{r},t)\pm\delta r\partial_i I_a(\mathbf{r},t)+\frac{1}{2}\delta r^2\partial_i^2 I_a(\mathbf{r},t)+o(\delta r^2)$, the first terms in the right-hand side of the PDEs become $(\epsilon/2)\delta r^2\partial_i^2 I_a(\mathbf{r},t)$ and $(\epsilon/2)\delta r^2\partial_i^2 S_a(\mathbf{r},t)$ up to the second order. For other terms, zeroth-order contributions dominate for $\delta r\to0$. By

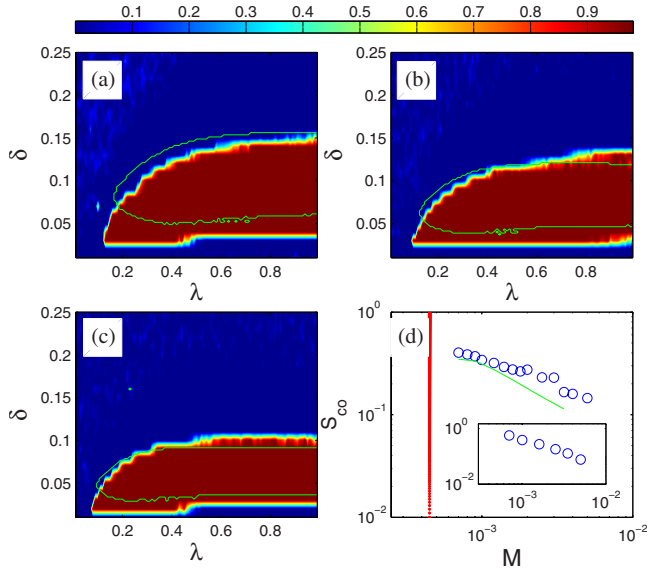

FIG. 2. (Color online) Under intraspecies virus spreading, survival probability (defined as the fraction of survival times in a number of independent realizations) in the λ-δ-parameter space for (a) $M=9\times10^{-4}$, (b) $M=1.2\times10^{-3}$, and (c) $M=1.6\times10^{-3}$, all larger than M_c. In all cases, a sizable coexistence area appears. The green curves are the predicted boundary of the coexistence area from Eq. (7). (d) Area of coexistence region S_{co} as a function of M ($N=200\times200$ for inset), where the red vertical line represents M_c and the green curve is obtained from Eq. (7). The quantity S_{co} is approximately an algebraic function of M, and slowly decreases as M increases. The lattice size except the inset in (d) is 100×100 and each point in the two-parameter space is obtained by averaging over 50 different realizations.

rescaling the exchange rate ϵ with the system size N according to $\epsilon=2MN^{0.5}$, we have $\epsilon\delta r^2=2M$. We thus obtain the following set of PDEs:

$$\partial_t I_a = M\nabla^2 I_a + \alpha\psi_a S_a - \beta I_a - uI_a\rho_c;$$

$$\partial_t S_a = M\nabla^2 S_a - \alpha\psi_a S_a - uS_a\rho_c + \sigma\rho_a(1-\rho);$$

$$\partial_t I_b = M\nabla^2 I_b + \alpha\psi_b S_b - \beta I_b - uI_b\rho_a;$$

$$\partial_t S_b = M\nabla^2 S_b - \alpha\psi_b S_b - uS_b\rho_a + \sigma\rho_b(1-\rho);$$

$$\partial_t I_c = M\nabla^2 I_c + \alpha\psi_c S_c - \beta I_c - uI_c\rho_b;$$

$$\partial_t S_c = M\nabla^2 S_c - \alpha\psi_c S_c - uS_c\rho_b + \sigma\rho_c(1-\rho); \qquad (7)$$

where for intra- and interspecies transmissions $\psi_{a,b,c}=I_{a,b,c}$ and $\psi_{a,b,c}=I_a+I_b+I_c$, respectively. Given the initial densities of infected and susceptible species and empty sites, as well as the values of λ and δ, we can numerically solve the PDE system to obtain patterns in Figs. 1(e)–1(h), which show a good agreement with direct numerical simulations.

Figures 2(a)–2(d) show two-parameter phase diagrams of the survival probability in the presence of intraspecies infection for different values of M in the regime $M>M_c$. We see that, regardless of the choice of M, a coexistence region always exists [Figs. 2(a)–2(c)], defined as the region where the survival probabilities of all three species are one. The coexistent region in the parameter space can be well predicted by our PDE formulation. Considering that, in the absence of virus spreading, coexistence cannot occur, these results indicate that intraspecies spreading can promote coexistence in a wide region of the parameter space. The area of the coexistence parameter region thus provides a way to characterize the strength of species coexistence for different values of M. As shown in Fig. 2(d), the area S_{co} of the coexistence region is approximately an algebraic function of M, and S_{co} decreases slowly as M is increased. In contrast, for interspecies virus spreading, there is no coexistence region for $M>M_c$, as verified by both direct simulation and PDEs.

The mechanism underlying the effect of intra- and interspecies spreading on coexistence can be heuristically explained by relating these processes to intraspecies competition such as $AA\rightarrow A\emptyset$ and natural death $A\rightarrow\emptyset$, respectively. Intraspecies spreading, which is somewhat similar to intraspecies competition, is most effective on the dominant subpopulation due to propagation, thereby reducing its predominance. This naturally favors coexistence. The empty sites resulting from death also act as topological defects that can help prevent extinction. The process of interspecies spreading resembles natural death if the infection probability is high. However, the barrier effect by natural death is not sufficient to sustain coexistence, so in general interspecies spreading cannot facilitate coexistence.

We now study basins of coexistence and extinction to provide a more comprehensive picture for the effects of virus spreading. Since the initial densities of three species satisfy $\rho_a+\rho_b+\rho_c=1-\rho_e$ (ρ_e being the density of empty sites), for a fixed value of ρ_e, all possible combinations of ρ_a, ρ_b, and ρ_c can be represented by a triangular region, the simplex S_2. There are four possible final states, corresponding to three single species (uniform) and coexistence. Thus, in the phase space S_2, the coordinates of a point represent a group of three initial densities, and the color of the point denotes the final state. As shown in Fig. 3(a), in the absence of virus spreading, for $M>M_c$, we obtain three uniform basins that are symmetrical and spirally entangled at the center. However, in the presence of intraspecies spreading, for the same value of M, a vast coexistence basin predominates S_2 with small basins near the borders for extinction, indicating the robustness of coexistence as induced by intraspecies spreading, regardless of the heterogeneity in the initial population densities. This is a remarkable feature as, intuitively, population heterogeneity is thought to be disadvantageous to species coexistence. For interspecies infection, no coexistence basin can arise, as shown in Fig. 3(c) (solution from PDEs) and Fig. 3(d) (direct numerical simulations). An observation from Fig. 3(c) is that the initial density ρ_e of empty sites does not change the structure of the uniform basin, but merely shrinks the area of the simplex S_2. Under intraspecies virus spreading, for very large value of M, the uniform (extinction) basin appears to be determined by λ and δ but not by M. For a fixed value of M in this regime, we show in Fig. 4 the structures of the uniform basins, which are distinct for different values of λ and δ. The basins exhibit some interesting features. For example, for $\delta=0.01$, when λ is changed from 0.01

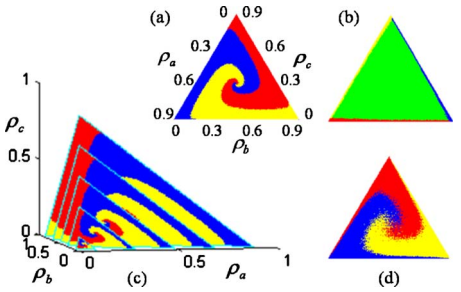

FIG. 3. (Color online) Basin structures in the simplex S_2 for $M=1.0\times10^{-3}>M_c$. (a) Spirally entangled basins of three species in the absence of virus spreading. (b) Rising of a vast area of coexistence (green) as a result of intraspecies spreading. (c) Theoretically predicted basin structures from Eq. (7) under interspecies spreading for different values of initial density ρ_e of empty sites. (d) Simulated basin structure under interspecies spreading. In (a,b,d), the value of ρ_e is fixed at 0.1. The color at each location represents the final state obtained from stochastic simulations by using 50 random realizations, under the same initial condition. Infection and death probabilities are $\lambda=0.6$ and $\delta=0.13$, respectively. The lattice size is 100×100. For the PDEs, extinction is defined when the density of any species is less than $1/N$. The species preyed by the extinction species is the exclusive survivor. The definition takes into account the physical meaning of survival in that the number of survival species cannot be less than one.

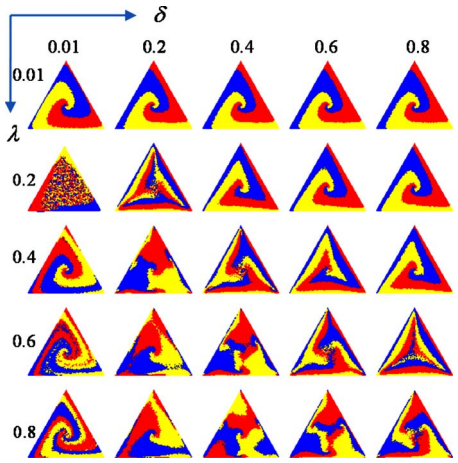

FIG. 4. (Color online) Structures of uniform basins in the presence of intraspecies infection as functions of infection parameters λ and δ for $M=3\times10^{-3}>M_c$. Data points in each simplex S_2 are obtained by averaging over 50 realizations. The color coding and other parameters are the same as in Fig. 3. All basin structures are rotationally symmetric and are insensitive to mobility for $M>M_c$.

to 0.4, the basins appear clockwise. For $\delta=0.01$ and $\lambda=0.2$, there is a large entangled region where small deviations in the initial composition could lead to completely different behavior. Although the structures can be dramatically changed with respect to δ and λ, the rotational symmetry is always preserved.

In conclusion, we have investigated the effects of intra- and interspecies virus spreading on species coexistence in spatial rock-paper-scissors game of mobile individuals. A striking finding is that intraspecies spreading can strongly promote coexistence in that robust coexistence basin can arise in parameter regimes where coexistence is ruled out in the absence of spreading. In contrast, interspecies spreading is not able to promote coexistence. We have derived a set of nonlinear PDEs incorporating both types of spreading process, and the theoretically predicted basin structures agree well with those from direct simulations. We speculate that intraspecies virus spreading can be a fundamental mechanism for species coexistence and biodiversity in nature.

This work was supported by AFOSR under Grant No. FA9550-10-1-0083, by a seed grant from the National Academies Keck Futures Initiative (NAKFI) on Complex Systems, by BBSRC under Grants No. BB-F00513X and No. BB-G010722, and by the Scottish Northern Research Partnership.

[1] B. Kerr, M. A. Riley, M. W. Feldman, and B. J. M. Bohannan, Nature (London) **418**, 171 (2002).
[2] T. L. Czárán, R. F. Hoekstra, and L. Pagie, Proc. Natl. Acad. Sci. U.S.A. **99**, 786 (2002).
[3] Y.-C. Lai and Y.-R. Liu, Phys. Rev. Lett. **94**, 038102 (2005).
[4] A. Traulsen, J. C. Claussen, and C. Hauert Phys. Rev. Lett. **95**, 238701 (2005); Phys. Rev. E **74**, 011901 (2006); J. C. Claussen and A. Traulsen, Phys. Rev. Lett. **100**, 058104 (2008).
[5] G. Szabó and G. Fáth, Phys. Rep. **446**, 97 (2007).
[6] M. Berr, T. Reichenbach, M. Schottenloher, and E. Frey, Phys. Rev. Lett. **102**, 048102 (2009).
[7] J. B. C. Jackson and L. Buss, Proc. Natl. Acad. Sci. U.S.A. **72**, 5160 (1975).
[8] C. E. Paquin and J. Adams, Nature (London) **306**, 368 (1983).
[9] B. Sinervo and C. M. Lively, Nature (London) **380**, 240 (1996).
[10] G. Szabó, J. Phys. A **38**, 6689 (2005); G. Szabó and G. A. Sznaider, Phys. Rev. E **69**, 031911 (2004); G. Szabó, A. Szolnoki, and G. A. Sznaider, *ibid.* **76**, 051921 (2007); G. Szabó, A. Szolnoki, and I. Borsos, *ibid.* **77**, 041919 (2008).
[11] T. Reichenbach, M. Mobilia, and E. Frey, Nature (London) **448**, 1046 (2007).
[12] T. Reichenbach, M. Mobilia, and E. Frey, Phys. Rev. Lett. **99**, 238105 (2007).
[13] T. Reichenbach, M. Mobilia, and E. Frey, J. Theor. Biol. **254**, 368 (2008).
[14] T. Reichenbach and E. Frey, Phys. Rev. Lett. **101**, 058102 (2008).
[15] M. Peltomäki and M. Alava, Phys. Rev. E **78**, 031906 (2008).
[16] H. Shi, W.-X. Wang, R. Yang, and Y.-C. Lai, Phys. Rev. E **81**, 030901(R) (2010).
[17] See, for example, M. Boguñá, R. Pastor-Satorras, and A. Vespignani, Phys. Rev. Lett. **90**, 028701 (2003); V. Colizza, A. Barrat, M. Barthelemy, and A. Vespignani, Proc. Natl. Acad. Sci. U.S.A. **103**, 2015 (2006); BMC Med. **5**, 34 (2007).
[18] S. Redner, *A Guide to First-Passage Processes* (Cambridge University Press, Cambridge, England, 2001).